https://doi.org/10.1016/j.mechmachtheory.2019.103637

Different Kinds of 3*T*2*R* Serial Kinematic Chains and Their Applications in Synthesis of Parallel Mechanisms

Shuofei Yang, Yangmin Li[1,2,*]

[1]The Hong Kong Polytechnic University, Department of Industrial and Systems Engineering, Kowloon, Hong Kong 999077, China

[2]Tianjin Key Laboratory for Advanced Mechatronic System Design and Intelligent Control, Tianjin University of Technology, Tianjin 300384, China

Abstract: This paper proposes a new three-translational and two-rotational (3*T*2*R*) motion with one fixed and one variable rotation directions. The serial kinematic chains (SKCs) that generate this motion are synthesized, which are quite different from the SKCs generating 3*T*2*R* motion with two fixed rotation directions. Firstly, according to the relationships between the two rotations in a motion, the classification of 3*T*2*R* motions is discussed. By using finite screw as the mathematical tool, the expressions of the two different kinds of 3*T*2*R* motions are formulated as algebraic sets. Secondly, serial motion generators of the 3*T*2*R* motions are investigated. The SKCs that generate the first-kind 3*T*2*R* motion are briefly reviewed; the twenty-eight types of SKCs that generate the second-kind 3*T*2*R* motion are synthesized by analytical derivations. Finally, the SKCs with the second-kind 3*T*2*R* motion are used to synthesize new parallel mechanisms. Two five-degree-of-freedom (five-DoF) systematical parallel mechanisms are taken as examples to show the applications of these SKCs. This paper provides theoretical foundations for the research on motions generated by complex SKCs and on motion patterns with variable rotation directions and centers.

Keywords: Mechanism synthesis, Serial kinematic chains, Parallel mechanisms, Screw theory

1. Introduction

The investigation on motion characteristics of serial kinematic chains (SKCs) is an important topic in the research of mechanism synthesis [1-2]. In-deep understanding of similarities and differences among various SKCs is the theoretical base of SKC synthesis. It also provides foundation for type synthesis of parallel mechanisms because SKCs serve as limbs of parallel mechanisms [3-6].

In recent years, many kinds of SKCs have been studied including the ones with single operation mode and the ones with multiple operation modes [7-10]. Among them, the SKCs with three-translational and two-rotational (3*T*2*R*) motion attract a lot of interests, which have been utilized in the synthesis of different kinds of parallel mechanisms. These 3*T*2*R* SKCs have the same motion pattern. Each of them can generate translations along arbitrary directions and rotations around two fixed directions. The 3*T*2*R* motion of these SKCs is named as double-Schoenflies motion [11]. SKCs with this 3*T*2*R* motion have been well discussed and synthesized through using different methods, such as the displacement manifold method [12-15], the virtual chain method [7, 16, 17], and the finite screw method [18, 19], and so on. The obtained 3*T*2*R* SKCs were used in type synthesis of parallel mechanisms having 3*T* motion [14, 16, 18], the ones having 3*T*1*R* Schoenflies motion [15, 17], bifurcation of Schoenflies motion [12], motion with variable rotational axis [19], and the ones having 3*T*2*R* double-Schoenflies motion [13]. These parallel mechanisms have good performances and wide applications, which shows the importance of these 3*T*2*R* SKCs.

In this commonly studied 3*T*2*R* motion with two fixed directions of rotations, the rotational directions have no influences on each other, and the translations can only change the positions of the rotational axes. In other words, the two rotations are independent with each other, and they are independent with the translations in the same time. Inspired by the motion of Exechon parallel mechanism [20] in which the direction of one rotation is determined by the direction and rotational angle of the other one, we propose another kind of 3*T*2*R* motion in this paper. A mechanism with the new 3*T*2*R* motion can generate three-DoF translations and two-DoF rotations in terms of finite motions from its specific initial pose, and the mechanism generates a rotation about an axis with fixed direction followed by another rotation whose axis has variable direction. Different from the Exechon motion, the variable rotation in this 3*T*2*R* motion has the following characteristics. 1) The direction vector of the variable rotation is not only determined by the direction and rotational angle of the fixed rotation, but also determined by the three-DoF translations. 2) The position vector of the variable rotation can be arbitrarily changed by the translations. The detailed comparison between the variable rotations in this new motion and the Exechon motion can be referred to the following Table.

Table 1 Comparison between the variable rotations in the new 3*T*2*R* motion and Exechon motion

	Variable rotation in the new 3*T*2*R* motion		Variable rotation in the 1*T*2*R* Exechon motion	
	Direction	Position	Direction	Position
Influenced by the fixed rotation	√	×	√	×
Influenced by the translation(s)	√	√	×	×

*Corresponding Author: yangmin.li@polyu.edu.hk

Based upon the existing $3T2R$ motion with two fixed rotational directions and inspired by the Exechon motion, a new kind of $3T2R$ motion with one fixed and one variable rotational directions is investigated in this paper. We use finite screw in quasi-vector form as mathematical tool [21, 22], because it is a simple and concise format for motion analysis and mechanism synthesis [23-27]. In the meantime, the kinematic [28-32], dynamic [33-35], accuracy [36, 37], stiffness [38-41] analysis and control [42-44] of the synthesized mechanisms can be easily carried out using the instantaneous screw [45-49] which is the counterpart of finite screw.

The outline of this paper is as follows: A brief review of the state-of-the-art of the research on the traditional $3T2R$ SKCs is conducted, and the basic concepts of a new $3T2R$ motion are introduced in Section 1. In Section 2, the classification of $3T2R$ motions is further discussed, and the two different kinds of $3T2R$ motions are expressed in form of finite screw sets. In Section 3, SKCs which are motion generators of the first-kind $3T2R$ motion are briefly reviewed; the SKCs generating the second-kind $3T2R$ motion are detailedly synthesized by analytical derivations, which results in twenty-eight structures of SKCs. The usage and applications of the SKCs with the second-kind $3T2R$ motion in the synthesis of new parallel mechanisms are shown in Section 4 through two examples. The conclusions of the paper are drawn in Section 5.

2. Different kinds of $3T2R$ motions

In this paper, we use finite screw as the mathematical tool because it has been proved to be the simplest format for finite motion description [21]. Here, we briefly introduce the finite screw method.

A rigid body motion can be generally expressed by a finite screw as

$$\boldsymbol{S}_f = 2\tan\frac{\theta}{2}\begin{pmatrix} \boldsymbol{s}_f \\ \boldsymbol{r}_f \times \boldsymbol{s}_f \end{pmatrix} + t\begin{pmatrix} \boldsymbol{0} \\ \boldsymbol{s}_f \end{pmatrix}, \tag{1}$$

where $\begin{pmatrix} \boldsymbol{s}_f^{\mathrm{T}} & (\boldsymbol{r}_f \times \boldsymbol{s}_f)^{\mathrm{T}} \end{pmatrix}^{\mathrm{T}}$ denotes the Chasles' axis of the motion that has the three-dimensional vectors $\boldsymbol{s}_f$ ($|\boldsymbol{s}_f| = 1$) and $\boldsymbol{r}_f$ as its direction and position vectors; θ and t are the rotational angle about that axis and the translational distance along the axis, respectively.

In this way, one-degree-of freedom (one-DoF) pure rotation and one-DoF pure translation can be respectively expressed as

$$\boldsymbol{S}_f = \begin{cases} 2\tan\dfrac{\theta}{2}\begin{pmatrix} \boldsymbol{s}_f \\ \boldsymbol{r}_f \times \boldsymbol{s}_f \end{pmatrix} & \text{pure rotation} \\ t\begin{pmatrix} \boldsymbol{0} \\ \boldsymbol{s}_f \end{pmatrix} = \begin{pmatrix} \boldsymbol{0} \\ \boldsymbol{t} \end{pmatrix} & \text{pure translation} \end{cases}, \tag{2}$$

where $\boldsymbol{t}$ is the substitution of $t\boldsymbol{s}_f$, which denotes the total translation vector.

Following this manner, the rotations generated by a revolute (R) joint and the translations generated by a prismatic (P) joint can be respectively expressed by the sets of finite screws as

$$\{\boldsymbol{S}_f\} = \begin{cases} \left\{ 2\tan\dfrac{\theta_{\mathrm{R}}}{2}\begin{pmatrix} \boldsymbol{s}_{\mathrm{R}} \\ \boldsymbol{r}_{\mathrm{R}} \times \boldsymbol{s}_{\mathrm{R}} \end{pmatrix} \middle| \theta_{\mathrm{R}} \in [0, 2\pi] \right\} & \text{R joint} \\ \left\{ t_{\mathrm{P}}\begin{pmatrix} \boldsymbol{0} \\ \boldsymbol{s}_{\mathrm{P}} \end{pmatrix} \middle| t_{\mathrm{P}} \in \mathbb{R} \right\} & \text{P joint} \end{cases}, \tag{3}$$

where $\boldsymbol{s}_{\mathrm{R}}$ ($|\boldsymbol{s}_{\mathrm{R}}| = 1$) and $\boldsymbol{r}_{\mathrm{R}}$ denote the direction and position vectors of the R joint's axis, and θ_{R} is the rotational angle of the joint; $\boldsymbol{s}_{\mathrm{P}}$ ($|\boldsymbol{s}_{\mathrm{P}}| = 1$) denotes the direction vector of the P joint, and t_{P} is the translational distance of the joint. Here, without loss of generality, we suppose that the value ranges of θ_{R} and t_{P} are $[0, 2\pi]$ and $\mathbb{R}$ (the real number field), respectively.

Through using the composition algorithm of finite screws, i.e., screw triangle product, the multi-DoF motion that is the composition of several motions or the motion generated by a SKC consisting of several R and P joints can be expressed as

$$\{\boldsymbol{S}_{f,\mathrm{SKC}}\} = \left\{ \boldsymbol{S}_{f,n} \triangle \cdots \triangle \boldsymbol{S}_{f,2} \triangle \boldsymbol{S}_{f,1} \middle| \theta_i \in [0, 2\pi],\ t_i \in \mathbb{R},\ i = 1, 2, \cdots, n \right\}, \tag{4}$$

where $\boldsymbol{S}_{f,1}$, $\boldsymbol{S}_{f,2}$, and $\boldsymbol{S}_{f,n}$ are finite screws having θ_i and t_i ($i = 1, 2, \cdots, n$) as the parameters; "$\triangle$" denotes the screw triangle product. The details algorithms of this product can be referred to the [21].

Based upon the relationship between the two rotations in a motion, the 3*T*2*R* motions can be classified into two kinds. The two rotations in the first-kind motion have fixed directions. The basic expression for the motion is

$$
\begin{aligned}
\left\{\boldsymbol{S}_{f,3T2R}^{1}\right\} &= \left\{2\tan\frac{\theta_b}{2}\begin{pmatrix}\boldsymbol{s}_b\\ \boldsymbol{r}_b\times\boldsymbol{s}_b\end{pmatrix}\triangle 2\tan\frac{\theta_a}{2}\begin{pmatrix}\boldsymbol{s}_a\\ \boldsymbol{r}_a\times\boldsymbol{s}_a\end{pmatrix}\triangle t_3\begin{pmatrix}\mathbf{0}\\ \boldsymbol{s}_3\end{pmatrix}\triangle t_2\begin{pmatrix}\mathbf{0}\\ \boldsymbol{s}_2\end{pmatrix}\triangle t_1\begin{pmatrix}\mathbf{0}\\ \boldsymbol{s}_1\end{pmatrix}\middle|\begin{array}{l}\theta_a,\theta_b\in[0,2\pi],\\ t_1,t_2,t_3\in\mathbb{R}\end{array}\right\} \\
&= \left\{2\tan\frac{\theta_b}{2}\begin{pmatrix}\boldsymbol{s}_b\\ \boldsymbol{r}_b\times\boldsymbol{s}_b\end{pmatrix}\triangle 2\tan\frac{\theta_a}{2}\begin{pmatrix}\boldsymbol{s}_a\\ \boldsymbol{r}_a\times\boldsymbol{s}_a\end{pmatrix}\triangle\begin{pmatrix}\mathbf{0}\\ t_3\boldsymbol{s}_3+t_2\boldsymbol{s}_2+t_1\boldsymbol{s}_1\end{pmatrix}\right\}
\end{aligned}, \tag{5}
$$

where $\boldsymbol{s}_b$ and $\boldsymbol{s}_a$ are the two fixed directions of the rotations; the position vectors of the rotations can be arbitrarily selected because of the influence from the three translations; $\boldsymbol{s}_1$, $\boldsymbol{s}_2$, and $\boldsymbol{s}_3$ are three independent directions of the translations. $\theta\,(t)$ with specific subscript denotes the corresponding rotational angle (translational distance) about (along) the direction $\boldsymbol{s}$ with the same subscript.

The two rotations in the second-kind motion have one fixed direction and one variable direction, the basic expression for the motion is

$$
\begin{aligned}
\left\{\boldsymbol{S}_{f,3T2R}^{2}\right\} &= \left\{2\tan\frac{\theta_b}{2}\begin{pmatrix}\boldsymbol{s}_b\\ \boldsymbol{r}_b\times\boldsymbol{s}_b\end{pmatrix}\triangle 2\tan\frac{\theta_a}{2}\begin{pmatrix}\exp\left(\theta_{b,1}\left[\boldsymbol{s}_b\times\right]\right)\boldsymbol{s}_a\\ \boldsymbol{r}_a\times\exp\left(\theta_{b,1}\left[\boldsymbol{s}_b\times\right]\right)\boldsymbol{s}_a\end{pmatrix}\triangle t_3\begin{pmatrix}\mathbf{0}\\ \boldsymbol{s}_3\end{pmatrix}\triangle t_2\begin{pmatrix}\mathbf{0}\\ \boldsymbol{s}_2\end{pmatrix}\triangle t_1\begin{pmatrix}\mathbf{0}\\ \boldsymbol{s}_1\end{pmatrix}\middle|\begin{array}{l}\theta_a,\theta_b\in[0,2\pi],\\ t_1,t_2,t_3\in\mathbb{R}\end{array}\right\} \\
&= \left\{2\tan\frac{\theta_b}{2}\begin{pmatrix}\boldsymbol{s}_b\\ \boldsymbol{r}_b\times\boldsymbol{s}_b\end{pmatrix}\triangle 2\tan\frac{\theta_a}{2}\begin{pmatrix}\exp\left(\theta_{b,1}\left[\boldsymbol{s}_b\times\right]\right)\boldsymbol{s}_a\\ \boldsymbol{r}_a\times\exp\left(\theta_{b,1}\left[\boldsymbol{s}_b\times\right]\right)\boldsymbol{s}_a\end{pmatrix}\triangle\begin{pmatrix}\mathbf{0}\\ t_3\boldsymbol{s}_3+t_2\boldsymbol{s}_2+t_1\boldsymbol{s}_1\end{pmatrix}\right\}
\end{aligned}, \tag{6}
$$

where $\boldsymbol{s}_b$ is the fixed direction, while $\exp\left(\theta_{b,1}\left[\boldsymbol{s}_b\times\right]\right)\boldsymbol{s}_a$ is the changing direction; $\left[\boldsymbol{s}_b\times\right]$ denotes the skew-symmetric matrix of vector $\boldsymbol{s}_b$ that represents its cross product. Similar with the first-kind 3*T*2*R* motion, the position vectors of the rotations can be arbitrarily selected because of the influence from the three translations, and $\boldsymbol{s}_1$, $\boldsymbol{s}_2$, $\boldsymbol{s}_3$ are three independent directions of the translations.

In both Eq. (5) and Eq. (6), θ_a, θ_b, t_1, t_2, and t_3 are the five independent parameters. This means that, in Eq. (6), $\theta_{b,1}$ is not an independent parameter, which depends on the five independent parameters. The relationship between $\theta_{b,1}$ and θ_a, θ_b, t_1, t_2, t_3 is determined by the specific structure of the serial kinematic chain that generates the second-kind 3*T*2*R* motion. Due to the three-DoF translations, the specific values of the two position vectors of the rotations in Eqs. (5) and (6), $\boldsymbol{r}_b$ and $\boldsymbol{r}_a$, have no influences on $\left\{\boldsymbol{S}_{f,3T2R}^{1}\right\}$ and $\left\{\boldsymbol{S}_{f,3T2R}^{2}\right\}$. In other words, $\boldsymbol{r}_b$ and $\boldsymbol{r}_a$ can be arbitrarily selected, i.e., $\boldsymbol{r}_b\in\mathbb{R}^3$ and $\boldsymbol{r}_a\in\mathbb{R}^3$.

3. 3*T*2*R* serial kinematic chains

After having discussed the two kinds of 3*T*2*R* motions in Section 2, the SKCs that generate each kind of motions will be investigated in this section. These SKCs are named as serial motion generators of the motions. Here-in-after, we call the SKCs as motion generators for simplicity.

3.1 Motion generators of the first-kind 3*T*2*R* motion

The first-kind 3*T*2*R* motion is the traditional one which has been widely discussed. Through using the computational properties of finite screw, the whole set of SKCs that generate this motion has been synthesized in the existing works, as listed in the following Table.

Table 2 Motion generators of the first-kind 3*T*2*R* motion

No.	SKC	No.	SKC	No.	SKC	No.	SKC
1	$P_1P_2P_3R_aR_b$	2	$P_1P_2R_aP_3R_b$	3	$P_1R_aP_2P_3R_b$	4	$R_aP_1P_2P_3R_b$
5	$P_1P_2R_aR_bP_3$	6	$P_1R_aP_2R_bP_3$	7	$R_aP_1P_2R_bP_3$	8	$P_1R_aR_bP_2P_3$
9	$R_aP_1R_bP_2P_3$	10	$R_aR_bP_1P_2P_3$	11	$P_1P_2R_aR_aR_b$	12	$P_1R_aP_2R_aR_b$
13	$P_1R_aR_aP_2R_b$	14	$P_1R_aR_aR_bP_2$	15	$R_aP_1P_2R_aR_b$	16	$R_aP_1R_aP_2R_b$
17	$R_aP_1R_aR_bP_2$	18	$R_aR_aP_1P_2R_b$	19	$R_aR_aP_1R_bP_2$	20	$R_aR_aR_bP_1P_2$
21	$P_1P_2R_aR_bR_b$	22	$P_1R_aP_2R_bR_b$	23	$P_1R_aR_bP_2R_b$	24	$P_1R_aR_bR_bP_2$
25	$R_aP_1P_2R_bR_b$	26	$R_aP_1R_bP_2R_b$	27	$R_aP_1R_bR_bP_2$	28	$R_aR_bP_1P_2R_b$
29	$R_aR_bP_1R_bP_2$	30	$R_aR_bR_bP_1P_2$	31	$P_1R_aR_aR_aR_b$	32	$R_aP_1R_aR_aR_b$
33	$R_aR_aP_1R_aR_b$	34	$R_aR_aR_aP_1R_b$	35	$R_aR_aR_aR_bP_1$	36	$P_1R_aR_bR_bR_b$
37	$R_aP_1R_bR_bR_b$	38	$R_aR_bP_1R_bR_b$	39	$R_aR_bR_bP_1R_b$	40	$R_aR_bR_bR_bP_1$
41	$P_1R_aR_aR_bR_b$	42	$R_aP_1R_aR_bR_b$	43	$R_aR_aP_1R_bR_b$	44	$R_aR_aR_bP_1R_b$

45	$R_aR_aR_bR_bP_1$	46	$R_aR_aR_aR_bR_b$	47	$R_aR_aR_bR_bR_b$

The geometrical conditions for these SKCs are:

(1) In each SKC from Nos. 11 to 30, the two P joints are not both perpendicular to the direction of the dyad of two parallel R joints.

(2) In each SKC from Nos. 31 to 40, the P joint is not perpendicular to the direction of the triad of three parallel R joints.

Regardless of the dimensions of the links in the SKCs, each SKC in Table 2 generates the 3*T*2*R* motion that is equivalent with the motion in Eq. (5). Some SKCs (Nos. 1, 11, 31, 41, and 46) generating the first-kind 3*T*2*R* motion are shown in Fig. 1. Without loss of generality, in Fig. 1, we suppose that the P_2 and R_a joints have the same directions, and that the P_3 and R_b joints have the same directions.

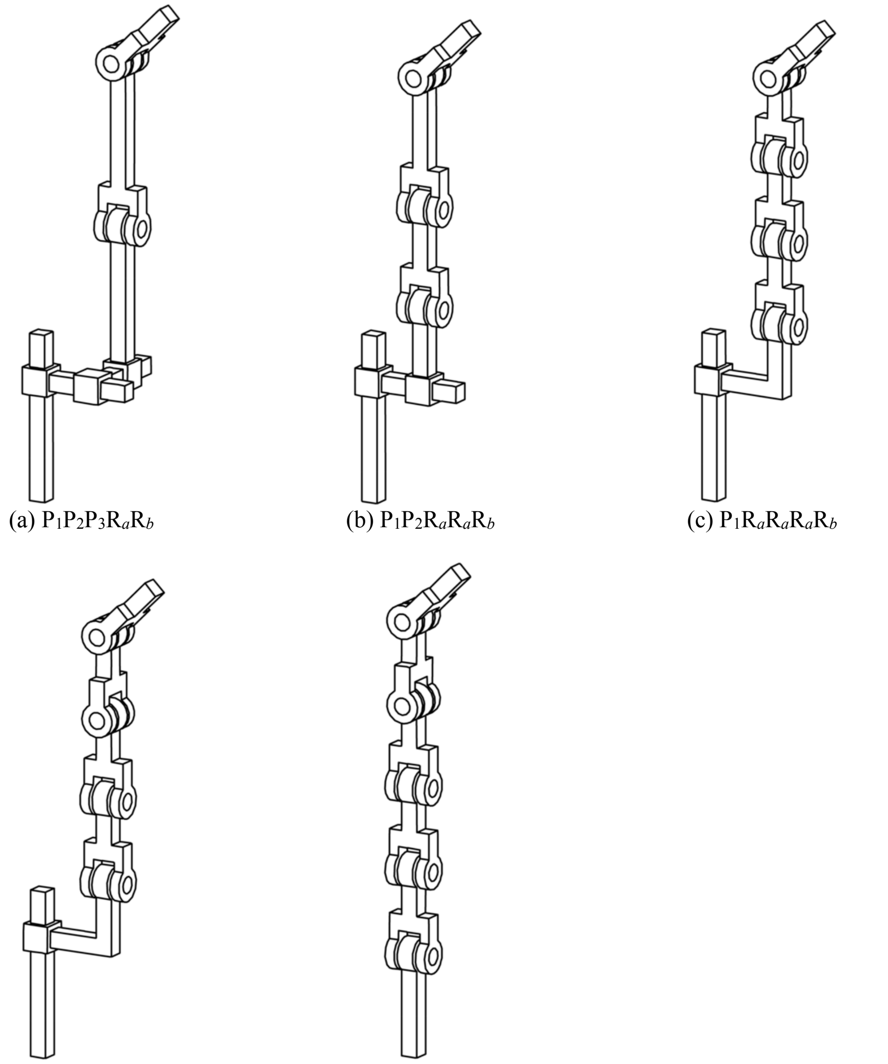

(a) $P_1P_2P_3R_aR_b$ (b) $P_1P_2R_aR_aR_b$ (c) $P_1R_aR_aR_aR_b$

(d) $P_1R_aR_aR_bR_b$ (e) $R_aR_aR_aR_bR_b$

Fig. 1 The SKCs generating the first-kind 3*T*2*R* motion

3.2 Motion generators of the second-kind 3*T*2*R* motion

It can be easily observed from Table 2 that for a SKC that generates the first-kind 3*T*2*R* motion, there is no R_a joint between two parallel R_b joints. In other words, there are no sub-structures like "$R_bR_aR_b$", "$R_bR_aR_aR_b$", and "$R_bR_aR_aR_aR_b$" in such a SKC. However, in SKCs generating the second-kind 3*T*2*R* motion, these sub-structures will exist, as discussed in this section.

In the following derivations, the subscripts of the symbols indicate the joints that they describe. For examples, $\boldsymbol{s}_a$ denotes the unit direction vector of an R_a joint; $\boldsymbol{r}_{a,1}$ denotes the position vector of the first R_a joint in a SKC; $\theta_{a,1}$ denotes the rotational angle of the first R_a joint in a SKC; $\boldsymbol{s}_1'$ denotes the unit direction vector of a P_1 joint; t_1' denotes the translational distance of a P_1 joint.

3.2.1 $P_1P_2R_bR_aR_b$ and its derivations

The most basic SKC that generates the second-kind 3*T*2*R* motion is $P_1P_2R_bR_aR_b$. According to Eq. (4), its motion expression is

$$\left\{\boldsymbol{S}_{f,\mathrm{P_1P_2R}_b\mathrm{R}_a\mathrm{R}_b}\right\}=\left\{2\tan\frac{\theta_{b,2}}{2}\begin{pmatrix}\boldsymbol{s}_b\\ \boldsymbol{r}_{b,2}\times\boldsymbol{s}_b\end{pmatrix}\triangle 2\tan\frac{\theta_a}{2}\begin{pmatrix}\boldsymbol{s}_a\\ \boldsymbol{r}_a'\times\boldsymbol{s}_a\end{pmatrix}\triangle 2\tan\frac{\theta_{b,1}}{2}\begin{pmatrix}\boldsymbol{s}_b\\ \boldsymbol{r}_{b,1}\times\boldsymbol{s}_b\end{pmatrix}\triangle t_2'\begin{pmatrix}\boldsymbol{0}\\ \boldsymbol{s}_2'\end{pmatrix}\triangle t_1'\begin{pmatrix}\boldsymbol{0}\\ \boldsymbol{s}_1'\end{pmatrix}\right\}, \tag{7}$$

where $(\boldsymbol{s}_1'\times\boldsymbol{s}_2')\times\boldsymbol{s}_b\neq\boldsymbol{0}$.

The above equation can be equivalently rewritten by using the properties of the screw triangle product, and the resultant expression is obtained as

$$\left\{\boldsymbol{S}_{f,\mathrm{P_1P_2R}_b\mathrm{R}_a\mathrm{R}_b}\right\}=\left\{\begin{array}{l}2\tan\dfrac{\theta_{b,1}+\theta_{b,2}}{2}\begin{pmatrix}\boldsymbol{s}_b\\ \boldsymbol{r}_{b,2}\times\boldsymbol{s}_b\end{pmatrix}\triangle 2\tan\dfrac{\theta_a}{2}\begin{pmatrix}\exp(\theta_{b,1}[\boldsymbol{s}_b\times])\boldsymbol{s}_a\\ (\boldsymbol{r}_{b,1}+\exp(\theta_{b,1}[\boldsymbol{s}_b\times])(\boldsymbol{r}_a'-\boldsymbol{r}_{b,1}))\times\exp(\theta_{b,1}[\boldsymbol{s}_b\times])\boldsymbol{s}_a\end{pmatrix}\\ \triangle\begin{pmatrix}\boldsymbol{0}\\ \exp(\theta_a[\boldsymbol{s}_a\times])(\exp(\theta_{b,1}[\boldsymbol{s}_b\times])-\boldsymbol{E}_3)(\boldsymbol{r}_{b,2}-\boldsymbol{r}_{b,1})+t_2'\boldsymbol{s}_2'+t_1'\boldsymbol{s}_1'\end{pmatrix}\end{array}\right\}, \tag{8}$$

where $\boldsymbol{E}_3$ denotes a three-order unit matrix.

It is easy to see that the following substitutions of symbols can be made in Eq. (8) without changing the value range of $\left\{\boldsymbol{S}_{f,\mathrm{P_1P_2R}_b\mathrm{R}_a\mathrm{R}_b}\right\}$, as

$$\theta_{b,1}+\theta_{b,2}\in[0,4\pi]\to\theta_b\in[0,2\pi],$$

$$\exp(\theta_a[\boldsymbol{s}_a\times])(\exp(\theta_{b,1}[\boldsymbol{s}_b\times])-\boldsymbol{E}_3)(\boldsymbol{r}_{b,2}-\boldsymbol{r}_{b,1})+t_2'\boldsymbol{s}_2'+t_1'\boldsymbol{s}_1'\in\mathbb{R}^3\to t_3\boldsymbol{s}_3+t_2\boldsymbol{s}_2+t_1\boldsymbol{s}_1\in\mathbb{R}^3,$$

$$\boldsymbol{r}_{b,2}\to\forall\boldsymbol{r}_b\in\mathbb{R}^3,\ \left(\boldsymbol{r}_{b,1}+\exp(\theta_{b,1}[\boldsymbol{s}_b\times])(\boldsymbol{r}_a'-\boldsymbol{r}_{b,1})\right)\to\forall\boldsymbol{r}_a\in\mathbb{R}^3.$$

In this way, Eq. (8) is proved to be equivalent with Eq. (6). And the relationship between $\theta_{b,1}$ and θ_a, t_1, t_2, t_3 of $\mathrm{P_1P_2R}_b\mathrm{R}_a\mathrm{R}_b$ can be derived from the following equation by using Euler's formula to rewrite $\exp(\theta_{b,1}[\boldsymbol{s}_b\times])$,

$$\left(\exp(\theta_{b,1}[\boldsymbol{s}_b\times])-\boldsymbol{E}_3\right)\left(\boldsymbol{r}_{b,2}-\boldsymbol{r}_{b,1}\right)^{\mathrm{T}}(\boldsymbol{s}_1'\times\boldsymbol{s}_2')=\exp(-\theta_a[\boldsymbol{s}_a\times])\left(t_3\boldsymbol{s}_3+t_2\boldsymbol{s}_2+t_1\boldsymbol{s}_1\right)^{\mathrm{T}}(\boldsymbol{s}_1'\times\boldsymbol{s}_2'). \tag{9}$$

The motion generators of the second-kind 3*T*2*R* motion that are similar with $\mathrm{P_1P_2R}_b\mathrm{R}_a\mathrm{R}_b$ are listed in Table 3 (containing $\mathrm{P_1P_2R}_b\mathrm{R}_a\mathrm{R}_b$).

Table 3 Motion generators of the second-kind 3*T*2*R* motion that are derived from $\mathrm{P_1P_2R}_b\mathrm{R}_a\mathrm{R}_b$

No.	SKC	Equation for deriving the relationship between $\theta_{b,1}$ and θ_a, θ_b, t_1, t_2, t_3
1	$\mathrm{P_1P_2R}_b\mathrm{R}_a\mathrm{R}_b$	$\boldsymbol{A}(\boldsymbol{B}_1-\boldsymbol{E}_3)(\boldsymbol{r}_{b,2}-\boldsymbol{r}_{b,1})+t_2'\boldsymbol{s}_2'+t_1'\boldsymbol{s}_1'=t_3\boldsymbol{s}_3+t_2\boldsymbol{s}_2+t_1\boldsymbol{s}_1$
2	$\mathrm{P_1R}_b\mathrm{P_2R}_a\mathrm{R}_b$	$\boldsymbol{A}(\boldsymbol{B}_1-\boldsymbol{E}_3)(\boldsymbol{r}_{b,2}-\boldsymbol{r}_{b,1})+t_2'\boldsymbol{B}_1\boldsymbol{s}_2'+t_1'\boldsymbol{s}_1'=t_3\boldsymbol{s}_3+t_2\boldsymbol{s}_2+t_1\boldsymbol{s}_1$
3	$\mathrm{P_1R}_b\mathrm{R}_a\mathrm{P_2R}_b$	$\boldsymbol{A}(\boldsymbol{B}_1-\boldsymbol{E}_3)(\boldsymbol{r}_{b,2}-\boldsymbol{r}_{b,1})+t_2'\boldsymbol{B}_1\boldsymbol{A}\boldsymbol{s}_2'+t_1'\boldsymbol{s}_1'=t_3\boldsymbol{s}_3+t_2\boldsymbol{s}_2+t_1\boldsymbol{s}_1$
4	$\mathrm{P_1R}_b\mathrm{R}_a\mathrm{R}_b\mathrm{P_2}$	$\boldsymbol{A}(\boldsymbol{B}_1-\boldsymbol{E}_3)(\boldsymbol{r}_{b,2}-\boldsymbol{r}_{b,1})+t_2'\boldsymbol{B}_1\boldsymbol{A}\boldsymbol{B}_2\boldsymbol{s}_2'+t_1'\boldsymbol{s}_1'=t_3\boldsymbol{s}_3+t_2\boldsymbol{s}_2+t_1\boldsymbol{s}_1$
5	$\mathrm{R}_b\mathrm{P_1P_2R}_a\mathrm{R}_b$	$\boldsymbol{A}(\boldsymbol{B}_1-\boldsymbol{E}_3)(\boldsymbol{r}_{b,2}-\boldsymbol{r}_{b,1})+\boldsymbol{B}_1(t_2'\boldsymbol{s}_2'+t_1'\boldsymbol{s}_1')=t_3\boldsymbol{s}_3+t_2\boldsymbol{s}_2+t_1\boldsymbol{s}_1$
6	$\mathrm{R}_b\mathrm{P_1R}_a\mathrm{P_2R}_b$	$\boldsymbol{A}(\boldsymbol{B}_1-\boldsymbol{E}_3)(\boldsymbol{r}_{b,2}-\boldsymbol{r}_{b,1})+t_2'\boldsymbol{B}_1\boldsymbol{A}\boldsymbol{s}_2'+t_1'\boldsymbol{B}_1\boldsymbol{s}_1'=t_3\boldsymbol{s}_3+t_2\boldsymbol{s}_2+t_1\boldsymbol{s}_1$
7	$\mathrm{R}_b\mathrm{P_1R}_a\mathrm{R}_b\mathrm{P_2}$	$\boldsymbol{A}(\boldsymbol{B}_1-\boldsymbol{E}_3)(\boldsymbol{r}_{b,2}-\boldsymbol{r}_{b,1})+t_2'\boldsymbol{B}_1\boldsymbol{A}\boldsymbol{B}_2\boldsymbol{s}_2'+t_1'\boldsymbol{B}_1\boldsymbol{s}_1'=t_3\boldsymbol{s}_3+t_2\boldsymbol{s}_2+t_1\boldsymbol{s}_1$
8	$\mathrm{R}_b\mathrm{R}_a\mathrm{P_1P_2R}_b$	$\boldsymbol{A}(\boldsymbol{B}_1-\boldsymbol{E}_3)(\boldsymbol{r}_{b,2}-\boldsymbol{r}_{b,1})+\boldsymbol{B}_1\boldsymbol{A}(t_2'\boldsymbol{s}_2'+t_1'\boldsymbol{s}_1')=t_3\boldsymbol{s}_3+t_2\boldsymbol{s}_2+t_1\boldsymbol{s}_1$
9	$\mathrm{R}_b\mathrm{R}_a\mathrm{P_1R}_b\mathrm{P_2}$	$\boldsymbol{A}(\boldsymbol{B}_1-\boldsymbol{E}_3)(\boldsymbol{r}_{b,2}-\boldsymbol{r}_{b,1})+t_2'\boldsymbol{B}_1\boldsymbol{A}\boldsymbol{s}_2'+t_1'\boldsymbol{B}_1\boldsymbol{A}\boldsymbol{B}_2\boldsymbol{s}_1'=t_3\boldsymbol{s}_3+t_2\boldsymbol{s}_2+t_1\boldsymbol{s}_1$
10	$\mathrm{R}_b\mathrm{R}_a\mathrm{R}_b\mathrm{P_1P_2}$	$\boldsymbol{A}(\boldsymbol{B}_1-\boldsymbol{E}_3)(\boldsymbol{r}_{b,2}-\boldsymbol{r}_{b,1})+\boldsymbol{B}_1\boldsymbol{A}\boldsymbol{B}_2(t_2'\boldsymbol{s}_2'+t_1'\boldsymbol{s}_1')=t_3\boldsymbol{s}_3+t_2\boldsymbol{s}_2+t_1\boldsymbol{s}_1$
Noted: $(\boldsymbol{s}_1'\times\boldsymbol{s}_2')\times\boldsymbol{s}_b\neq\boldsymbol{0}$, $\boldsymbol{A}=\exp(\theta_a[\boldsymbol{s}_a\times])$, $\boldsymbol{B}_1=\exp(\theta_{b,1}[\boldsymbol{s}_b\times])$, $\boldsymbol{B}_2=\exp((\theta_b-\theta_{b,1})[\boldsymbol{s}_b\times])$.		

In Table 3, for each SKC, the equation contains three scalar equations with three dependent parameters, $\theta_{b,1}$, t_1' and t_2', to be solved. These three parameters can be respectively solved as the expressions of the four/five independent parameters, θ_a, (θ_b,) t_1, t_2, t_3. Hence, the relationship between $\theta_{b,1}$ and these independent parameters can be derived from the equation.

3.2.2 P$_1$R$_b$R$_a$R$_a$R$_b$ and its derivations

Besides P$_1$P$_2$R$_b$R$_a$R$_b$ and its derivations, P$_1$R$_b$R$_a$R$_a$R$_b$ is also a motion generator of the second-kind 3*T*2*R* motion. The motion expression of this SKC is

$$\left\{\boldsymbol{S}_{f,\mathrm{P_1R}_b\mathrm{R}_a\mathrm{R}_a\mathrm{R}_b}\right\}=\left\{2\tan\frac{\theta_{b,2}}{2}\begin{pmatrix}\boldsymbol{s}_b\\ \boldsymbol{r}_{b,2}\times\boldsymbol{s}_b\end{pmatrix}\triangle 2\tan\frac{\theta_{a,2}}{2}\begin{pmatrix}\boldsymbol{s}_a\\ \boldsymbol{r}_{a,2}\times\boldsymbol{s}_a\end{pmatrix}\triangle 2\tan\frac{\theta_{a,1}}{2}\begin{pmatrix}\boldsymbol{s}_a\\ \boldsymbol{r}_{a,1}\times\boldsymbol{s}_a\end{pmatrix}\triangle 2\tan\frac{\theta_{b,1}}{2}\begin{pmatrix}\boldsymbol{s}_b\\ \boldsymbol{r}_{b,1}\times\boldsymbol{s}_b\end{pmatrix}\triangle t_1'\begin{pmatrix}\boldsymbol{0}\\ \boldsymbol{s}_1'\end{pmatrix}\right\},\quad(10)$$

which can be equivalently rewritten as

$$\left\{\boldsymbol{S}_{f,\mathrm{P_1R}_b\mathrm{R}_a\mathrm{R}_a\mathrm{R}_b}\right\}=\left\{\begin{array}{l}2\tan\dfrac{\theta_{b,1}+\theta_{b,2}}{2}\begin{pmatrix}\boldsymbol{s}_b\\ \boldsymbol{r}_{b,2}\times\boldsymbol{s}_b\end{pmatrix}\triangle 2\tan\dfrac{\theta_{a,1}+\theta_{a,2}}{2}\begin{pmatrix}\exp\left(\theta_{b,1}\left[\boldsymbol{s}_b\times\right]\right)\boldsymbol{s}_a\\ \left(\boldsymbol{r}_{b,1}+\exp\left(\theta_{b,1}\left[\boldsymbol{s}_b\times\right]\right)\left(\boldsymbol{r}_{a,2}-\boldsymbol{r}_{b,1}\right)\right)\times\exp\left(\theta_{b,1}\left[\boldsymbol{s}_b\times\right]\right)\boldsymbol{s}_a\end{pmatrix}\\ \triangle\begin{pmatrix}\boldsymbol{0}\\ \left(\begin{array}{l}\exp\left(\left(\theta_{a,1}+\theta_{a,2}\right)\left[\boldsymbol{s}_a\times\right]\right)\left(\exp\left(\theta_{b,1}\left[\boldsymbol{s}_b\times\right]\right)-\boldsymbol{E}_3\right)\left(\boldsymbol{r}_{b,2}-\boldsymbol{r}_{b,1}\right)\\ +\exp\left(\theta_{b,1}\left[\boldsymbol{s}_b\times\right]\right)\left(\exp\left(\theta_{a,1}\left[\boldsymbol{s}_a\times\right]\right)-\boldsymbol{E}_3\right)\left(\boldsymbol{r}_{a,2}-\boldsymbol{r}_{a,1}\right)+t_1'\boldsymbol{s}_1'\end{array}\right)\end{pmatrix}\end{array}\right\}.(11)$$

Without changing the value range of the above equation, the following substitutions of symbols can be made in it,

$$\theta_{b,1}+\theta_{b,2}\in[0,4\pi]\to\theta_b\in[0,2\pi],\ \ \theta_{a,1}+\theta_{a,2}\in[0,4\pi]\to\theta_a\in[0,2\pi],$$

$$\left(\begin{array}{l}\exp\left(\theta_a\left[\boldsymbol{s}_a\times\right]\right)\left(\exp\left(\theta_{b,1}\left[\boldsymbol{s}_b\times\right]\right)-\boldsymbol{E}_3\right)\left(\boldsymbol{r}_{b,2}-\boldsymbol{r}_{b,1}\right)\\ +\exp\left(\theta_{b,1}\left[\boldsymbol{s}_b\times\right]\right)\left(\exp\left(\theta_{a,1}\left[\boldsymbol{s}_a\times\right]\right)-\boldsymbol{E}_3\right)\left(\boldsymbol{r}_{a,2}-\boldsymbol{r}_{a,1}\right)+t_1'\boldsymbol{s}_1'\end{array}\right)\in\mathbb{R}^3\to t_3\boldsymbol{s}_3+t_2\boldsymbol{s}_2+t_1\boldsymbol{s}_1\in\mathbb{R}^3,$$

$$\boldsymbol{r}_{b,2}\to\forall\boldsymbol{r}_b\in\mathbb{R}^3,\ \ \left(\boldsymbol{r}_{b,1}+\exp\left(\theta_{b,1}\left[\boldsymbol{s}_b\times\right]\right)\left(\boldsymbol{r}_{a,2}-\boldsymbol{r}_{b,1}\right)\right)\to\forall\boldsymbol{r}_a\in\mathbb{R}^3.$$

Hence, the equivalence between Eq. (11) and Eq. (6) is proved. There are more SKCs that are similar with P$_1$R$_b$R$_a$R$_a$R$_b$ and generate the second-kind 3*T*2*R* motion, as listed in Table 4 (containing P$_1$R$_b$R$_a$R$_a$R$_b$).

Table 4 Motion generators of the second-kind 3*T*2*R* motion that are derived from P$_1$R$_b$R$_a$R$_a$R$_b$

No.	SKC	Equation for deriving the relationship between $\theta_{b,1}$ and θ_a, θ_b, t_1, t_2, t_3
1	P$_1$R$_b$R$_a$R$_a$R$_b$	$\boldsymbol{A}(\boldsymbol{B}_1-\boldsymbol{E}_3)(\boldsymbol{r}_{b,2}-\boldsymbol{r}_{b,1})+\boldsymbol{B}_1(\boldsymbol{A}_1-\boldsymbol{E}_3)(\boldsymbol{r}_{a,2}-\boldsymbol{r}_{a,1})+t_1'\boldsymbol{s}_1'=t_3\boldsymbol{s}_3+t_2\boldsymbol{s}_2+t_1\boldsymbol{s}_1$
2	R$_b$P$_1$R$_a$R$_a$R$_b$	$\boldsymbol{A}(\boldsymbol{B}_1-\boldsymbol{E}_3)(\boldsymbol{r}_{b,2}-\boldsymbol{r}_{b,1})+\boldsymbol{B}_1(\boldsymbol{A}_1-\boldsymbol{E}_3)(\boldsymbol{r}_{a,2}-\boldsymbol{r}_{a,1})+t_1'\boldsymbol{B}_1\boldsymbol{s}_1'=t_3\boldsymbol{s}_3+t_2\boldsymbol{s}_2+t_1\boldsymbol{s}_1$
3	R$_b$R$_a$P$_1$R$_a$R$_b$	$\boldsymbol{A}(\boldsymbol{B}_1-\boldsymbol{E}_3)(\boldsymbol{r}_{b,2}-\boldsymbol{r}_{b,1})+\boldsymbol{B}_1(\boldsymbol{A}_1-\boldsymbol{E}_3)(\boldsymbol{r}_{a,2}-\boldsymbol{r}_{a,1})+t_1'\boldsymbol{B}_1\boldsymbol{A}_1\boldsymbol{s}_1'=t_3\boldsymbol{s}_3+t_2\boldsymbol{s}_2+t_1\boldsymbol{s}_1$
4	R$_b$R$_a$R$_a$P$_1$R$_b$	$\boldsymbol{A}(\boldsymbol{B}_1-\boldsymbol{E}_3)(\boldsymbol{r}_{b,2}-\boldsymbol{r}_{b,1})+\boldsymbol{B}_1(\boldsymbol{A}_1-\boldsymbol{E}_3)(\boldsymbol{r}_{a,2}-\boldsymbol{r}_{a,1})+t_1'\boldsymbol{B}_1\boldsymbol{A}_1\boldsymbol{A}_2\boldsymbol{s}_1'=t_3\boldsymbol{s}_3+t_2\boldsymbol{s}_2+t_1\boldsymbol{s}_1$
5	R$_b$R$_a$R$_a$R$_b$P$_1$	$\boldsymbol{A}(\boldsymbol{B}_1-\boldsymbol{E}_3)(\boldsymbol{r}_{b,2}-\boldsymbol{r}_{b,1})+\boldsymbol{B}_1(\boldsymbol{A}_1-\boldsymbol{E}_3)(\boldsymbol{r}_{a,2}-\boldsymbol{r}_{a,1})+t_1'\boldsymbol{B}_1\boldsymbol{A}_1\boldsymbol{A}_2\boldsymbol{B}_2\boldsymbol{s}_1'=t_3\boldsymbol{s}_3+t_2\boldsymbol{s}_2+t_1\boldsymbol{s}_1$
Noted: $\boldsymbol{A}=\exp\left(\theta_a\left[\boldsymbol{s}_a\times\right]\right)$, $\boldsymbol{A}_1=\exp\left(\theta_{a,1}\left[\boldsymbol{s}_a\times\right]\right)$, $\boldsymbol{B}_1=\exp\left(\theta_{b,1}\left[\boldsymbol{s}_b\times\right]\right)$, $\boldsymbol{B}_2=\exp\left(\left(\theta_b-\theta_{b,1}\right)\left[\boldsymbol{s}_b\times\right]\right)$.		

For each SKC in Table 4, $\theta_{b,1}$, $\theta_{a,1}$ and t_1' are the three parameters in the corresponding equation that consists of three scalar equations. Thus, the equation leads to the relationship between $\theta_{b,1}$ and θ_a, (θ_b,) t_1, t_2, t_3.

3.2.3 P$_1$R$_b$R$_a$R$_b$R$_b$, P$_1$R$_b$R$_b$R$_b$R$_a$R$_b$, and their derivations

For P$_1$R$_b$R$_a$R$_b$R$_b$, its motion can be expressed as

$$\left\{\boldsymbol{S}_{f,\mathrm{P_1R}_b\mathrm{R}_a\mathrm{R}_b\mathrm{R}_b}\right\}=\left\{2\tan\frac{\theta_{b,3}}{2}\begin{pmatrix}\boldsymbol{s}_b\\ \boldsymbol{r}_{b,3}\times\boldsymbol{s}_b\end{pmatrix}\triangle 2\tan\frac{\theta_{b,2}}{2}\begin{pmatrix}\boldsymbol{s}_b\\ \boldsymbol{r}_{b,2}\times\boldsymbol{s}_b\end{pmatrix}\triangle 2\tan\frac{\theta_a}{2}\begin{pmatrix}\boldsymbol{s}_a\\ \boldsymbol{r}_a'\times\boldsymbol{s}_a\end{pmatrix}\triangle 2\tan\frac{\theta_{b,1}}{2}\begin{pmatrix}\boldsymbol{s}_b\\ \boldsymbol{r}_{b,1}\times\boldsymbol{s}_b\end{pmatrix}\triangle t_1'\begin{pmatrix}\boldsymbol{0}\\ \boldsymbol{s}_1'\end{pmatrix}\right\},\quad(12)$$

where $\boldsymbol{s}_1'^{\mathrm{T}}\boldsymbol{s}_b\neq 0$. Equivalent rewriting of this equation results in

$$\left\{\boldsymbol{S}_{f,\mathrm{P_1R}_b\mathrm{R}_a\mathrm{R}_b\mathrm{R}_b}\right\}=\left\{\begin{array}{l}2\tan\frac{\theta_{b,1}+\theta_{b,2}+\theta_{b,3}}{2}\begin{pmatrix}\boldsymbol{s}_b\\ \boldsymbol{r}_{b,3}\times\boldsymbol{s}_b\end{pmatrix}\triangle 2\tan\frac{\theta_a}{2}\begin{pmatrix}\exp\left(\theta_{b,1}\left[\boldsymbol{s}_b\times\right]\right)\boldsymbol{s}_a\\ \left(\boldsymbol{r}_{b,1}+\exp\left(\theta_{b,1}\left[\boldsymbol{s}_b\times\right]\right)\left(\boldsymbol{r}_a'-\boldsymbol{r}_{b,1}\right)\right)\times\exp\left(\theta_{b,1}\left[\boldsymbol{s}_b\times\right]\right)\boldsymbol{s}_a\end{pmatrix}\\ \triangle\begin{pmatrix}\boldsymbol{0}\\ \left(\exp\left(\theta_a\left[\boldsymbol{s}_a\times\right]\right)\left(\exp\left(\theta_{b,1}\left[\boldsymbol{s}_b\times\right]\right)-\boldsymbol{E}_3\right)\left(\boldsymbol{r}_{b,2}-\boldsymbol{r}_{b,1}\right)\right.\\ \left.+\exp\left(\theta_a\left[\boldsymbol{s}_a\times\right]\right)\left(\exp\left(\left(\theta_{b,1}+\theta_{b,2}\right)\left[\boldsymbol{s}_b\times\right]\right)-\boldsymbol{E}_3\right)\left(\boldsymbol{r}_{b,3}-\boldsymbol{r}_{b,2}\right)+t_1'\boldsymbol{s}_1'\right)\end{pmatrix}\end{array}\right\}. \tag{13}$$

The following substitutions of symbols made in Eq. (13) will not change its value range, which shows that Eq. (13) is equivalent with Eq. (6).

$$\theta_{b,1}+\theta_{b,2}+\theta_{b,3}\in[0,6\pi]\to\theta_b\in[0,2\pi],$$

$$\begin{pmatrix}\exp\left(\theta_a\left[\boldsymbol{s}_a\times\right]\right)\left(\exp\left(\theta_{b,1}\left[\boldsymbol{s}_b\times\right]\right)-\boldsymbol{E}_3\right)\left(\boldsymbol{r}_{b,2}-\boldsymbol{r}_{b,1}\right)\\ +\exp\left(\theta_a\left[\boldsymbol{s}_a\times\right]\right)\left(\exp\left(\left(\theta_{b,1}+\theta_{b,2}\right)\left[\boldsymbol{s}_b\times\right]\right)-\boldsymbol{E}_3\right)\left(\boldsymbol{r}_{b,3}-\boldsymbol{r}_{b,2}\right)+t_1'\boldsymbol{s}_1'\end{pmatrix}\in\mathbb{R}^3\to t_3\boldsymbol{s}_3+t_2\boldsymbol{s}_2+t_1\boldsymbol{s}_1\in\mathbb{R}^3,$$

$$\boldsymbol{r}_{b,3}\to\forall\boldsymbol{r}_b\in\mathbb{R}^3,\ \left(\boldsymbol{r}_{b,1}+\exp\left(\theta_{b,1}\left[\boldsymbol{s}_b\times\right]\right)\left(\boldsymbol{r}_a'-\boldsymbol{r}_{b,1}\right)\right)\to\forall\boldsymbol{r}_a\in\mathbb{R}^3.$$

For $\mathrm{P_1R}_b\mathrm{R}_b\mathrm{R}_a\mathrm{R}_b$, its motion expression is formulated as

$$\left\{\boldsymbol{S}_{f,\mathrm{P_1R}_b\mathrm{R}_b\mathrm{R}_a\mathrm{R}_b}\right\}=\left\{2\tan\frac{\theta_{b,3}}{2}\begin{pmatrix}\boldsymbol{s}_b\\ \boldsymbol{r}_{b,3}\times\boldsymbol{s}_b\end{pmatrix}\triangle 2\tan\frac{\theta_a}{2}\begin{pmatrix}\boldsymbol{s}_a\\ \boldsymbol{r}_a'\times\boldsymbol{s}_a\end{pmatrix}\triangle 2\tan\frac{\theta_{b,2}}{2}\begin{pmatrix}\boldsymbol{s}_b\\ \boldsymbol{r}_{b,2}\times\boldsymbol{s}_b\end{pmatrix}\triangle 2\tan\frac{\theta_{b,1}'}{2}\begin{pmatrix}\boldsymbol{s}_b\\ \boldsymbol{r}_{b,1}\times\boldsymbol{s}_b\end{pmatrix}\triangle t_1'\begin{pmatrix}\boldsymbol{0}\\ \boldsymbol{s}_1'\end{pmatrix}\right\}, \tag{14}$$

where $\boldsymbol{s}_1'^{\mathrm{T}}\boldsymbol{s}_b\neq 0$. This equation can be equivalently rewritten into

$$\left\{\boldsymbol{S}_{f,\mathrm{P_1R}_b\mathrm{R}_b\mathrm{R}_a\mathrm{R}_b}\right\}=\left\{\begin{array}{l}2\tan\frac{\theta_{b,1}'+\theta_{b,2}+\theta_{b,3}}{2}\begin{pmatrix}\boldsymbol{s}_b\\ \boldsymbol{r}_{b,3}\times\boldsymbol{s}_b\end{pmatrix}\\ \triangle 2\tan\frac{\theta_a}{2}\begin{pmatrix}\exp\left(\left(\theta_{b,1}'+\theta_{b,2}\right)\left[\boldsymbol{s}_b\times\right]\right)\boldsymbol{s}_a\\ \left(\boldsymbol{r}_{b,1}+\exp\left(\theta_{b,1}'\left[\boldsymbol{s}_b\times\right]\right)\left(\boldsymbol{r}_{b,2}-\boldsymbol{r}_{b,1}+\exp\left(\theta_{b,2}\left[\boldsymbol{s}_b\times\right]\right)\left(\boldsymbol{r}_a'-\boldsymbol{r}_{b,2}\right)\right)\right)\\ \times\exp\left(\left(\theta_{b,1}'+\theta_{b,2}\right)\left[\boldsymbol{s}_b\times\right]\right)\boldsymbol{s}_a\end{pmatrix}\\ \triangle\begin{pmatrix}\boldsymbol{0}\\ \left(\exp\left(\theta_a\left[\boldsymbol{s}_a\times\right]\right)\left(\exp\left(\theta_{b,1}'\left[\boldsymbol{s}_b\times\right]\right)-\boldsymbol{E}_3\right)\left(\boldsymbol{r}_{b,2}-\boldsymbol{r}_{b,1}\right)\right.\\ \left.+\exp\left(\theta_a\left[\boldsymbol{s}_a\times\right]\right)\left(\exp\left(\left(\theta_{b,1}'+\theta_{b,2}\right)\left[\boldsymbol{s}_b\times\right]\right)-\boldsymbol{E}_3\right)\left(\boldsymbol{r}_{b,3}-\boldsymbol{r}_{b,2}\right)+t_1'\boldsymbol{s}_1'\right)\end{pmatrix}\end{array}\right\}. \tag{15}$$

Through making the following substitutions of symbols in Eq. (15), we can see that the value range of $\left\{\boldsymbol{S}_{f,\mathrm{P_1R}_b\mathrm{R}_b\mathrm{R}_a\mathrm{R}_b}\right\}$ will not change. In this manner, Eq. (15) and Eq. (6) are verified to be equivalent with each other.

$$\theta_{b,1}'+\theta_{b,2}+\theta_{b,3}\in[0,6\pi]\to\theta_b\in[0,2\pi],\ \theta_{b,1}'+\theta_{b,2}\in[0,4\pi]\to\theta_{b,1}\in[0,2\pi],$$

$$\begin{pmatrix}\exp\left(\theta_a\left[\boldsymbol{s}_a\times\right]\right)\left(\exp\left(\left(\theta_{b,1}-\theta_{b,2}\right)\left[\boldsymbol{s}_b\times\right]\right)-\boldsymbol{E}_3\right)\left(\boldsymbol{r}_{b,2}-\boldsymbol{r}_{b,1}\right)\\ +\exp\left(\theta_a\left[\boldsymbol{s}_a\times\right]\right)\left(\exp\left(\theta_{b,1}\left[\boldsymbol{s}_b\times\right]\right)-\boldsymbol{E}_3\right)\left(\boldsymbol{r}_{b,3}-\boldsymbol{r}_{b,2}\right)+t_1'\boldsymbol{s}_1'\end{pmatrix}\in\mathbb{R}^3\to t_3\boldsymbol{s}_3+t_2\boldsymbol{s}_2+t_1\boldsymbol{s}_1\in\mathbb{R}^3,$$

$$\boldsymbol{r}_{b,3}\to\forall\boldsymbol{r}_b\in\mathbb{R}^3,\ \left(\boldsymbol{r}_{b,1}+\exp\left(\theta_{b,1}'\left[\boldsymbol{s}_b\times\right]\right)\left(\boldsymbol{r}_{b,2}-\boldsymbol{r}_{b,1}+\exp\left(\theta_{b,2}\left[\boldsymbol{s}_b\times\right]\right)\left(\boldsymbol{r}_a'-\boldsymbol{r}_{b,2}\right)\right)\right)\to\forall\boldsymbol{r}_a\in\mathbb{R}^3.$$

More SKCs can be obtained as the derivations of these two SKCs, which are also motion generators of the second-kind 3*T*2*R* motion, as listed in Table 5 (containing $\mathrm{P_1R}_b\mathrm{R}_a\mathrm{R}_b\mathrm{R}_b$) and Table 6 (containing $\mathrm{P_1R}_b\mathrm{R}_b\mathrm{R}_a\mathrm{R}_b$).

For each SKC in Table 5, the equation constituted by three scalar equations has $\theta_{b,1}$, $\theta_{b,2}$ and t_1' as the three parameters; and for each SKC in Table 6, the same situation occurs. Hence, the relationship between $\theta_{b,1}$ and θ_a, (θ_b,) t_1, t_2, t_3 can be derived from the equation.

Table 5 Motion generators of the second-kind 3*T*2*R* motion that are derived from P1R*b*R*a*R*b*R*b*

No.	SKC	Equation for deriving the relationship between $\theta_{b,1}$ and θ_a, θ_b, t_1, t_2, t_3
1	P1R*b*R*a*R*b*R*b*	$\boldsymbol{A}\left(\left(\boldsymbol{B}_1-\boldsymbol{E}_3\right)\left(\boldsymbol{r}_{b,2}-\boldsymbol{r}_{b,1}\right)+\left(\boldsymbol{B}_1\boldsymbol{B}_2-\boldsymbol{E}_3\right)\left(\boldsymbol{r}_{b,3}-\boldsymbol{r}_{b,2}\right)\right)+t_1'\boldsymbol{s}_1'=t_3\boldsymbol{s}_3+t_2\boldsymbol{s}_2+t_1\boldsymbol{s}_1$
2	R*b*P1R*a*R*b*R*b*	$\boldsymbol{A}\left(\left(\boldsymbol{B}_1-\boldsymbol{E}_3\right)\left(\boldsymbol{r}_{b,2}-\boldsymbol{r}_{b,1}\right)+\left(\boldsymbol{B}_1\boldsymbol{B}_2-\boldsymbol{E}_3\right)\left(\boldsymbol{r}_{b,3}-\boldsymbol{r}_{b,2}\right)\right)+\boldsymbol{B}_1t_1'\boldsymbol{s}_1'=t_3\boldsymbol{s}_3+t_2\boldsymbol{s}_2+t_1\boldsymbol{s}_1$
3	R*b*R*a*P1R*b*R*b*	$\boldsymbol{A}\left(\left(\boldsymbol{B}_1-\boldsymbol{E}_3\right)\left(\boldsymbol{r}_{b,2}-\boldsymbol{r}_{b,1}\right)+\left(\boldsymbol{B}_1\boldsymbol{B}_2-\boldsymbol{E}_3\right)\left(\boldsymbol{r}_{b,3}-\boldsymbol{r}_{b,2}\right)\right)+\boldsymbol{B}_1\boldsymbol{A}t_1'\boldsymbol{s}_1'=t_3\boldsymbol{s}_3+t_2\boldsymbol{s}_2+t_1\boldsymbol{s}_1$
4	R*b*R*a*R*b*P1R*b*	$\boldsymbol{A}\left(\left(\boldsymbol{B}_1-\boldsymbol{E}_3\right)\left(\boldsymbol{r}_{b,2}-\boldsymbol{r}_{b,1}\right)+\left(\boldsymbol{B}_1\boldsymbol{B}_2-\boldsymbol{E}_3\right)\left(\boldsymbol{r}_{b,3}-\boldsymbol{r}_{b,2}\right)\right)+\boldsymbol{B}_1\boldsymbol{A}\boldsymbol{B}_2t_1'\boldsymbol{s}_1'=t_3\boldsymbol{s}_3+t_2\boldsymbol{s}_2+t_1\boldsymbol{s}_1$
5	R*b*R*a*R*b*R*b*P1	$\boldsymbol{A}\left(\left(\boldsymbol{B}_1-\boldsymbol{E}_3\right)\left(\boldsymbol{r}_{b,2}-\boldsymbol{r}_{b,1}\right)+\left(\boldsymbol{B}_1\boldsymbol{B}_2-\boldsymbol{E}_3\right)\left(\boldsymbol{r}_{b,3}-\boldsymbol{r}_{b,2}\right)\right)+\boldsymbol{B}_1\boldsymbol{A}\boldsymbol{B}_2\boldsymbol{B}_3t_1'\boldsymbol{s}_1'=t_3\boldsymbol{s}_3+t_2\boldsymbol{s}_2+t_1\boldsymbol{s}_1$
Noted: $\boldsymbol{A}=\exp\left(\theta_a\left[\boldsymbol{s}_a\times\right]\right)$, $\boldsymbol{B}_1=\exp\left(\theta_{b,1}\left[\boldsymbol{s}_b\times\right]\right)$, $\boldsymbol{B}_2=\exp\left(\theta_{b,2}\left[\boldsymbol{s}_b\times\right]\right)$, $\boldsymbol{B}_3=\exp\left(\left(\theta_b-\theta_{b,1}-\theta_{b,2}\right)\left[\boldsymbol{s}_b\times\right]\right)$.		

Table 6 Motion generators of the second-kind 3*T*2*R* motion that are derived from P1R*b*R*b*R*a*R*b*

No.	SKC	Equation for deriving the relationship between $\theta_{b,1}$ and θ_a, θ_b, t_1, t_2, t_3
1	P1R*b*R*b*R*a*R*b*	$\boldsymbol{A}\left(\left(\boldsymbol{B}_1\boldsymbol{B}_2^{-1}-\boldsymbol{E}_3\right)\left(\boldsymbol{r}_{b,2}-\boldsymbol{r}_{b,1}\right)+\left(\boldsymbol{B}_1-\boldsymbol{E}_3\right)\left(\boldsymbol{r}_{b,3}-\boldsymbol{r}_{b,2}\right)\right)+t_1'\boldsymbol{s}_1'=t_3\boldsymbol{s}_3+t_2\boldsymbol{s}_2+t_1\boldsymbol{s}_1$
2	R*b*P1R*b*R*a*R*b*	$\boldsymbol{A}\left(\left(\boldsymbol{B}_1\boldsymbol{B}_2^{-1}-\boldsymbol{E}_3\right)\left(\boldsymbol{r}_{b,2}-\boldsymbol{r}_{b,1}\right)+\left(\boldsymbol{B}_1-\boldsymbol{E}_3\right)\left(\boldsymbol{r}_{b,3}-\boldsymbol{r}_{b,2}\right)\right)+\boldsymbol{B}_1\boldsymbol{B}_2^{-1}t_1'\boldsymbol{s}_1'=t_3\boldsymbol{s}_3+t_2\boldsymbol{s}_2+t_1\boldsymbol{s}_1$
3	R*b*R*b*P1R*a*R*b*	$\boldsymbol{A}\left(\left(\boldsymbol{B}_1\boldsymbol{B}_2^{-1}-\boldsymbol{E}_3\right)\left(\boldsymbol{r}_{b,2}-\boldsymbol{r}_{b,1}\right)+\left(\boldsymbol{B}_1-\boldsymbol{E}_3\right)\left(\boldsymbol{r}_{b,3}-\boldsymbol{r}_{b,2}\right)\right)+\boldsymbol{B}_1t_1'\boldsymbol{s}_1'=t_3\boldsymbol{s}_3+t_2\boldsymbol{s}_2+t_1\boldsymbol{s}_1$
4	R*b*R*b*R*a*P1R*b*	$\boldsymbol{A}\left(\left(\boldsymbol{B}_1\boldsymbol{B}_2^{-1}-\boldsymbol{E}_3\right)\left(\boldsymbol{r}_{b,2}-\boldsymbol{r}_{b,1}\right)+\left(\boldsymbol{B}_1-\boldsymbol{E}_3\right)\left(\boldsymbol{r}_{b,3}-\boldsymbol{r}_{b,2}\right)\right)+\boldsymbol{B}_1\boldsymbol{A}t_1'\boldsymbol{s}_1'=t_3\boldsymbol{s}_3+t_2\boldsymbol{s}_2+t_1\boldsymbol{s}_1$
5	R*b*R*b*R*a*R*b*P1	$\boldsymbol{A}\left(\left(\boldsymbol{B}_1\boldsymbol{B}_2^{-1}-\boldsymbol{E}_3\right)\left(\boldsymbol{r}_{b,2}-\boldsymbol{r}_{b,1}\right)+\left(\boldsymbol{B}_1-\boldsymbol{E}_3\right)\left(\boldsymbol{r}_{b,3}-\boldsymbol{r}_{b,2}\right)\right)+\boldsymbol{B}_1\boldsymbol{A}\boldsymbol{B}_3t_1'\boldsymbol{s}_1'=t_3\boldsymbol{s}_3+t_2\boldsymbol{s}_2+t_1\boldsymbol{s}_1$
Noted: $\boldsymbol{A}=\exp\left(\theta_a\left[\boldsymbol{s}_a\times\right]\right)$, $\boldsymbol{B}_1=\exp\left(\theta_{b,1}\left[\boldsymbol{s}_b\times\right]\right)$, $\boldsymbol{B}_2=\exp\left(\theta_{b,2}\left[\boldsymbol{s}_b\times\right]\right)$, $\boldsymbol{B}_3=\exp\left(\left(\theta_b-\theta_{b,1}\right)\left[\boldsymbol{s}_b\times\right]\right)$.		

3.2.4 R*b*R*a*R*a*R*b*R*b*, R*b*R*b*R*a*R*a*R*b*, and R*b*R*a*R*a*R*a*R*b*

For R*b*R*a*R*a*R*b*R*b*, its motion expression is obtained and rewritten as

$$\left\{\boldsymbol{S}_{f,\mathrm{R}_b\mathrm{R}_a\mathrm{R}_a\mathrm{R}_b\mathrm{R}_b}\right\}=\left\{\begin{array}{l}2\tan\dfrac{\theta_{b,3}}{2}\begin{pmatrix}\boldsymbol{s}_b\\ \boldsymbol{r}_{b,3}\times\boldsymbol{s}_b\end{pmatrix}\triangle 2\tan\dfrac{\theta_{b,2}}{2}\begin{pmatrix}\boldsymbol{s}_b\\ \boldsymbol{r}_{b,2}\times\boldsymbol{s}_b\end{pmatrix}\triangle 2\tan\dfrac{\theta_{a,2}}{2}\begin{pmatrix}\boldsymbol{s}_a\\ \boldsymbol{r}_{a,2}\times\boldsymbol{s}_a\end{pmatrix}\\ \triangle 2\tan\dfrac{\theta_{a,1}}{2}\begin{pmatrix}\boldsymbol{s}_a\\ \boldsymbol{r}_{a,1}\times\boldsymbol{s}_a\end{pmatrix}\triangle 2\tan\dfrac{\theta_{b,1}}{2}\begin{pmatrix}\boldsymbol{s}_b\\ \boldsymbol{r}_{b,1}\times\boldsymbol{s}_b\end{pmatrix}\end{array}\right\}, \tag{16}$$

and

$$\left\{\boldsymbol{S}_{f,\mathrm{R}_b\mathrm{R}_a\mathrm{R}_a\mathrm{R}_b\mathrm{R}_b}\right\}=\left\{\begin{array}{l}2\tan\dfrac{\theta_{b,1}+\theta_{b,2}+\theta_{b,3}}{2}\begin{pmatrix}\boldsymbol{s}_b\\ \boldsymbol{r}_{b,3}\times\boldsymbol{s}_b\end{pmatrix}\\ \triangle 2\tan\dfrac{\theta_{a,1}+\theta_{a,2}}{2}\begin{pmatrix}\exp\left(\theta_{b,1}\left[\boldsymbol{s}_b\times\right]\right)\boldsymbol{s}_a\\ \left(\boldsymbol{r}_{b,1}+\exp\left(\theta_{b,1}\left[\boldsymbol{s}_b\times\right]\right)\left(\boldsymbol{r}_{a,2}-\boldsymbol{r}_{b,1}\right)\right)\times\exp\left(\theta_{b,1}\left[\boldsymbol{s}_b\times\right]\right)\boldsymbol{s}_a\end{pmatrix}\\ \triangle\begin{pmatrix}\boldsymbol{0}\\ \left(\exp\left(\left(\theta_{a,1}+\theta_{a,2}\right)\left[\boldsymbol{s}_a\times\right]\right)\left(\exp\left(\theta_{b,1}\left[\boldsymbol{s}_b\times\right]\right)-\boldsymbol{E}_3\right)\left(\boldsymbol{r}_{b,2}-\boldsymbol{r}_{b,1}\right)\right.\\ +\exp\left(\left(\theta_{a,1}+\theta_{a,2}\right)\left[\boldsymbol{s}_a\times\right]\right)\left(\exp\left(\left(\theta_{b,1}+\theta_{b,2}\right)\left[\boldsymbol{s}_b\times\right]\right)-\boldsymbol{E}_3\right)\left(\boldsymbol{r}_{b,3}-\boldsymbol{r}_{b,2}\right)\\ \left.+\exp\left(\theta_{b,1}\left[\boldsymbol{s}_b\times\right]\right)\left(\exp\left(\theta_{a,1}\left[\boldsymbol{s}_a\times\right]\right)-\boldsymbol{E}_3\right)\left(\boldsymbol{r}_{a,2}-\boldsymbol{r}_{a,1}\right)\right)\end{pmatrix}\end{array}\right\}. \tag{17}$$

Through using the following substitutions, we can prove the equivalence between Eq. (16) and Eq. (6),

$$\theta_{b,1}+\theta_{b,2}+\theta_{b,3}\in\left[0,6\pi\right]\rightarrow\theta_b\in\left[0,2\pi\right],\quad \theta_{a,1}+\theta_{a,2}\in\left[0,4\pi\right]\rightarrow\theta_a\in\left[0,2\pi\right]$$

$$\begin{pmatrix} \exp\left(\theta_a\left[\boldsymbol{s}_a\times\right]\right)\left(\exp\left(\theta_{b,1}\left[\boldsymbol{s}_b\times\right]\right)-\boldsymbol{E}_3\right)\left(\boldsymbol{r}_{b,2}-\boldsymbol{r}_{b,1}\right) \\ +\exp\left(\theta_a\left[\boldsymbol{s}_a\times\right]\right)\left(\exp\left(\left(\theta_{b,1}+\theta_{b,2}\right)\left[\boldsymbol{s}_b\times\right]\right)-\boldsymbol{E}_3\right)\left(\boldsymbol{r}_{b,3}-\boldsymbol{r}_{b,2}\right) \\ +\exp\left(\theta_{b,1}\left[\boldsymbol{s}_b\times\right]\right)\left(\exp\left(\theta_{a,1}\left[\boldsymbol{s}_a\times\right]\right)-\boldsymbol{E}_3\right)\left(\boldsymbol{r}_{a,2}-\boldsymbol{r}_{a,1}\right) \end{pmatrix} \in \mathbb{R}^3 \to t_3\boldsymbol{s}_3+t_2\boldsymbol{s}_2+t_1\boldsymbol{s}_1 \in \mathbb{R}^3,$$

$$\boldsymbol{r}_{b,3} \to \forall \boldsymbol{r}_b \in \mathbb{R}^3,\ \left(\boldsymbol{r}_{b,1}+\exp\left(\theta_{b,1}\left[\boldsymbol{s}_b\times\right]\right)\left(\boldsymbol{r}_{a,2}-\boldsymbol{r}_{b,1}\right)\right) \to \forall \boldsymbol{r}_a \in \mathbb{R}^3.$$

The three dependent parameters, $\theta_{b,1}$, $\theta_{b,2}$, $\theta_{a,1}$, can be solved as the expressions of the four independent parameters, θ_a, t_1, t_2, t_3, through solving the following equation, which leads to the relationship between $\theta_{b,1}$ and θ_a, t_1, t_2, t_3,

$$\boldsymbol{A}\left(\boldsymbol{B}_1-\boldsymbol{E}_3\right)\left(\boldsymbol{r}_{b,2}-\boldsymbol{r}_{b,1}\right)+\boldsymbol{A}\left(\boldsymbol{B}_1\boldsymbol{B}_2-\boldsymbol{E}_3\right)\left(\boldsymbol{r}_{b,3}-\boldsymbol{r}_{b,2}\right)+\boldsymbol{B}_1\left(\boldsymbol{A}_1-\boldsymbol{E}_3\right)\left(\boldsymbol{r}_{a,2}-\boldsymbol{r}_{a,1}\right)=t_3\boldsymbol{s}_3+t_2\boldsymbol{s}_2+t_1\boldsymbol{s}_1, \tag{18}$$

where $\boldsymbol{A}=\exp\left(\theta_a\left[\boldsymbol{s}_a\times\right]\right)$, $\boldsymbol{A}_1=\exp\left(\theta_{a,1}\left[\boldsymbol{s}_a\times\right]\right)$, $\boldsymbol{B}_1=\exp\left(\theta_{b,1}\left[\boldsymbol{s}_b\times\right]\right)$, $\boldsymbol{B}_2=\exp\left(\theta_{b,2}\left[\boldsymbol{s}_b\times\right]\right)$.

Similar analysis can be conducted for $R_bR_bR_aR_aR_b$ and $R_bR_aR_aR_aR_b$ to prove the equivalences between their motion expressions and Eq. (6). Here, we do not give the details due to the space limitation.

Through the above analysis and derivations, all the twenty-eight motion generators of the second-kind 3*T*2*R* motion that have structures of SKCs are obtained. Several ones among them are shown in Fig. 2.

Fig. 2 shows the initial poses of these SKCs. Here, without loss of generality, we suppose that the P_2 and R_a joints have the same directions.

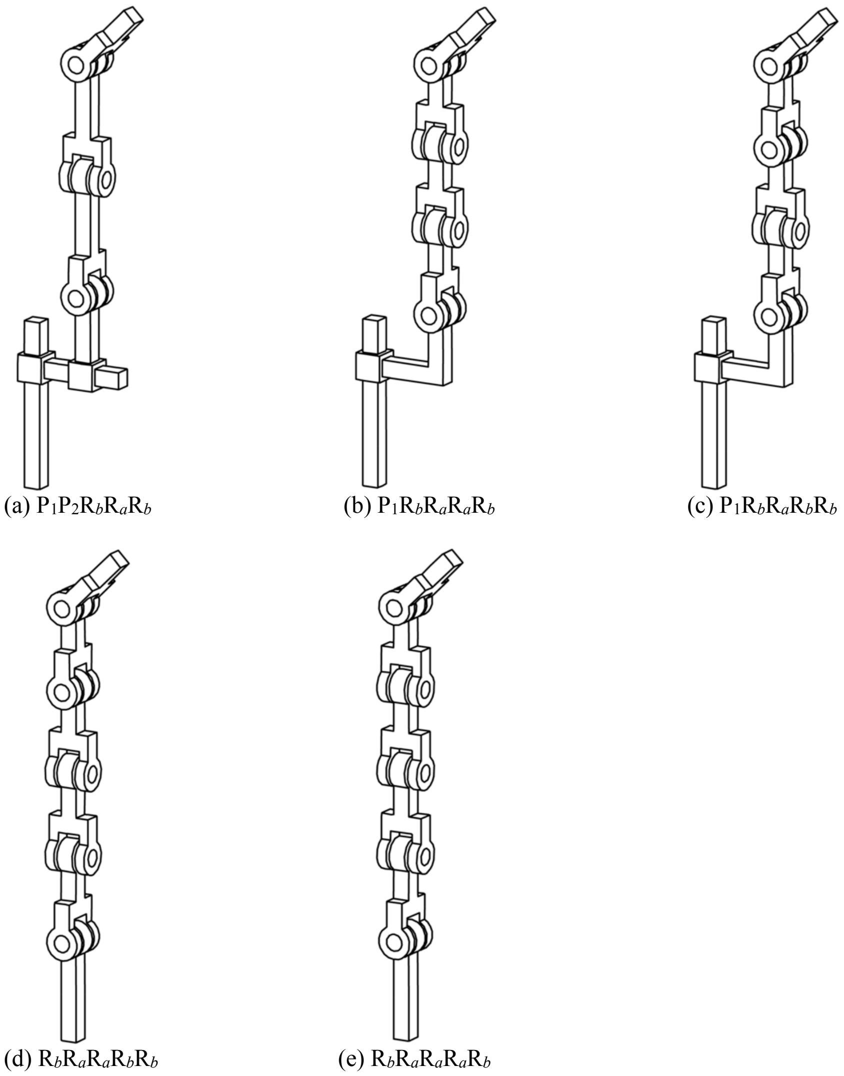

(a) $P_1P_2R_bR_aR_b$ (b) $P_1R_bR_aR_aR_b$ (c) $P_1R_bR_aR_bR_b$

(d) $R_bR_aR_aR_bR_b$ (e) $R_bR_aR_aR_aR_b$

Fig. 2 The SKCs generating the second-kind 3*T*2*R* motion

4. Synthesis of some new parallel mechanisms

The SKCs generating the first-kind $3T2R$ motion have been widely used in the type synthesis of parallel mechanisms, as discussed in Section 1. However, the SKCs that generate the second-kind $3T2R$ motion have not been paid much attention in the existing works for the following reasons:

(1) The second-kind $3T2R$ motion is hardly to be described by other methods. It is definitely defined and accurately expressed for the first time in this paper by using finite screw as the mathematical tool.

(2) The two kinds of $3T2R$ motions have not been reported to be distinguished. The SKCs generating the second-kind $3T2R$ motion are regarded to be motion equivalence with the ones generating the first-kind motion.

In this section, we will give two examples to show the usage of the SKCs generating the second-kind $3T2R$ motion in synthesis of new parallel mechanisms.

4.1 Example A

In this example, an $R_bR_aP_1R_aR_b$ SKC and five six-DoF UPS SKCs are used to constitute a five-DoF parallel mechanism. Here, U and S denote a universal and a spherical joint, respectively. There are two groups of adjacent R joints in the $R_bR_aP_1R_aR_b$ SKC, i.e., "R_bR_a" and "R_aR_b". Suppose that the "R_bR_a" has common rotational center, and so does the "R_aR_b". In this manner, the $R_bR_aP_1R_aR_b$ is equivalent to a UPU. Thus, the parallel mechanism with six limbs can be denoted as $R_bR_aP_1R_aR_b$-5-UPS or UPU-5-UPS.

The UPU limb connects the centers of the fixed base and the moving platform, and the five UPS limbs are arranged symmetrically around the UPU. In order to realize symmetric and non-redundant actuation arrangements, the five P joints in the five UPS limbs are selected as the actuation joints. The UPU limb provides the only constraint to the five-DoF parallel mechanism. The initial pose of mechanism is shown in Fig. 3.

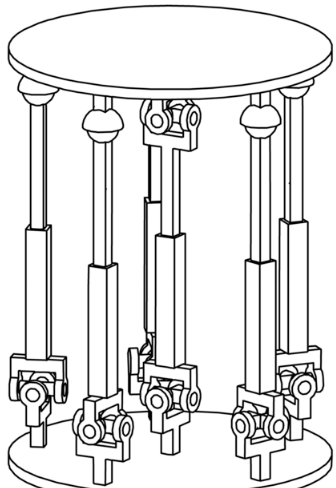

Fig. 3 A UPU-5-UPS parallel mechanism

Because each UPS generates the six-DoF motion, its motion can be expressed by the whole set of finite screws [21] regardless of the dimensions, as

$$\left\{\boldsymbol{S}_{f,\mathrm{UPS}}\right\}=\left\{2\tan\frac{\theta}{2}\begin{pmatrix}\boldsymbol{s}\\ \boldsymbol{r}\times\boldsymbol{s}\end{pmatrix}+t\begin{pmatrix}\boldsymbol{0}\\ \boldsymbol{s}\end{pmatrix}\middle|\,\theta\in[0,2\pi],\ t\in\mathbb{R},\ \boldsymbol{s}\in\mathbb{R}^3,\ |\boldsymbol{s}|=1,\ \boldsymbol{r}\in\mathbb{R}^3\right\}. \tag{19}$$

As a parallel mechanism' motion is the intersection of the motions of all its limbs, the motion of this parallel mechanism is obtained as

$$\begin{aligned}\left\{\boldsymbol{S}_{f,\mathrm{PM},1}\right\}&=\left\{\boldsymbol{S}_{f,\mathrm{UPU}}\right\}\cap\underbrace{\left\{\boldsymbol{S}_{f,\mathrm{UPS}}\right\}\cap\cdots\cap\left\{\boldsymbol{S}_{f,\mathrm{UPS}}\right\}}_{5}\\ &=\left\{\boldsymbol{S}_{f,\mathrm{R}_b\mathrm{R}_a\mathrm{P}_1\mathrm{R}_a\mathrm{R}_b}\right\}\\ &=\left\{2\tan\frac{\theta_{b,2}}{2}\begin{pmatrix}\boldsymbol{s}_b\\ \boldsymbol{r}_B\times\boldsymbol{s}_b\end{pmatrix}\triangle 2\tan\frac{\theta_{a,2}}{2}\begin{pmatrix}\boldsymbol{s}_a\\ \boldsymbol{r}_B\times\boldsymbol{s}_a\end{pmatrix}\triangle t_1\begin{pmatrix}\boldsymbol{0}\\ \boldsymbol{s}_1\end{pmatrix}\triangle 2\tan\frac{\theta_{a,1}}{2}\begin{pmatrix}\boldsymbol{s}_a\\ \boldsymbol{r}_A\times\boldsymbol{s}_a\end{pmatrix}\triangle 2\tan\frac{\theta_{b,1}}{2}\begin{pmatrix}\boldsymbol{s}_b\\ \boldsymbol{r}_A\times\boldsymbol{s}_b\end{pmatrix}\right\}\end{aligned}, \tag{20}$$

where $\boldsymbol{r}_A$ is the position vector of the common rotation center of the first U joint (R_bR_a), and $\boldsymbol{r}_B$ is the position vector of the common rotational center of the second U joint (R_aR_b).

Thus, the mechanism has the same $3T2R$ motion with its UPU ($R_bR_aP_1R_bR_b$) limb.

4.2 Example B

If five identical SKCs that generate the second-kind 3*T*2*R* motions are used as limbs, a new parallel mechanism with the same 3*T*2*R* motion will be synthesized. For instance, a parallel mechanism composed by five $R_bR_aP_1R_aR_b$ limbs is shown in Fig. 4. The five limbs are arranged symmetrically. We denote each limb as UPU by supposing that the adjacent R_a and R_b joints share the same rotational center. In this way, the parallel mechanism is denoted as 5-$R_bR_aP_1R_aR_b$ or 5-UPU.

At the initial pose of the parallel mechanism shown in Fig. 4, it should be noted that all the R_a joints in the five limbs of mechanism have the same direction, so do all the R_b joints. The five limbs provide identical constraints to the moving platform of the mechanism. Hence, the mechanism is an over-constrained one. The symmetric and non-redundant actuation arrangements for the mechanism are realized by selecting the five P joints as the actuation joints.

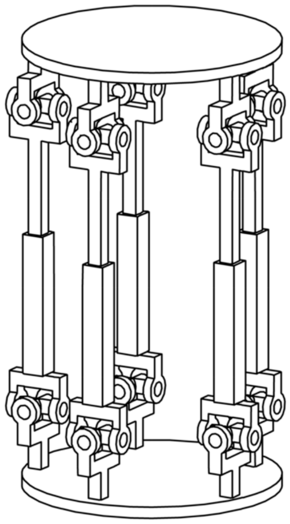

Fig. 4 A 5-UPU parallel mechanism

The motion of the parallel mechanism is the same as that of each $R_bR_aP_1R_aR_b$, as

$$\begin{aligned}\left\{\boldsymbol{S}_{f,\mathrm{PM},2}\right\} &= \underbrace{\left\{\boldsymbol{S}_{f,\mathrm{R}_b\mathrm{R}_a\mathrm{P}_1\mathrm{R}_a\mathrm{R}_b}\right\}\cap\cdots\cap\left\{\boldsymbol{S}_{f,\mathrm{R}_b\mathrm{R}_a\mathrm{P}_1\mathrm{R}_a\mathrm{R}_b}\right\}}_{5}, \\ &= \left\{\boldsymbol{S}_{f,\mathrm{R}_b\mathrm{R}_a\mathrm{P}_1\mathrm{R}_a\mathrm{R}_b}\right\}\end{aligned} \tag{21}$$

which is equivalent with Eq. (20).

Both the new parallel mechanisms in the two examples illustrated in this section generate the same motion with their five-DoF limbs. They can be regarded as the parallel motion generators of the second-kind 3*T*2*R* motions. Since they have one fixed and one variable rotation axes, they are quite different with the existing 3*T*2*R* parallel mechanisms with double-Schoenflies motion. Following the similar manner, more parallel mechanisms as well as single closed-loop mechanisms can be synthesized using the SKCs obtained in Section 3.2 as limbs. Here, we only give these two parallel mechanisms for example.

5. Conclusions

Inspired by the 3*T*2*R* motion with two fixed rotation directions and the 1*T*2*R* Exechon motion with one fixed and one variable rotation directions, this paper is focused on the synthesis of SKCs that generates a new 3*T*2*R* motion. The following conclusions are drawn.

(1) Two kinds of 3*T*2*R* motions are classified based upon the relationships between the rotation directions in a motion. The second-kind motion is proposed and expressed in this paper for the first time.

(2) All the SKCs that are motion generators of the second-kind 3*T*2*R* motion are synthesized through algebraic derivations of finite screw sets.

(3) Two new symmetrical parallel mechanisms are taken as examples to show that the synthesized SKCs have wide applications in the synthesis of parallel mechanisms.

Compared with the mechanisms having the first-kind 3*T*2*R* motion, the mechanisms having the second-kind 3*T*2*R* motion have more flexible rotation capabilities because each mechanism has a variable rotational direction. Therefore, the SKCs with the second-kind 3*T*2*R* motion have great potential to be deigned as the industrial robots for painting, welding, and palletizing, because they have more diversified orientation workspaces. This paper provides theoretical foundations for analyzing the motions generated by complex SKCs and synthesizing the mechanisms whose motion patterns have variable rotational directions and centers.

Acknowledgments

This research work was supported in part by the research project of the Research Committee of The Hong Kong Polytechnic University [Grant No. 1-ZE97]; in part by and General Research Fund (GRF) of the Research Grants Council (RGC) of Hong Kong, China [Grant No. PolyU 152137/19E]; in part by the National Natural Science Foundation of China (NSFC) [Grant Nos. 51575544 and 51875391]; and in part by Natural Science Foundation of Tianjin City [Grant No. 16JCZDJC38000].

References

[1] L.W. Tsai, Robot Analysis: The Mechanics of Serial and Parallel Manipulators, John Wiley & Sons, Inc., New York, 1999.

[2] X.M. Huo, T. Sun, Y.M. Song, et al., An analytical approach to determine motions/constraints of serial kinematic chains based on Clifford algebra, Proceedings of the Institution of Mechanical Engineers, Part C: Journal of Mechanical Engineering Science 231 (7) (2017) 1324-1338.

[3] Z. Huang, Q.C. Li, H.F. Ding, Theory of Parallel Mechanisms, Springer, Dordrecht, 2013

[4] Y. Qi, T. Sun, Y.M. Song, Type synthesis of parallel tracking mechanism with varied axes by modeling its finite motions algebraically, ASME Journal of Mechanisms and Robotics 9 (5) (2017) 054504-1-054504-6.

[5] T. Sun, Y.M. Song, H. Gao, et al, Topology synthesis of a 1-translational and 3-rotational parallel manipulator with an articulated traveling plate, ASME Journal of Mechanisms and Robotics 7 (3) (2015) 031015-1-031015-9.

[6] Y. Qi, T. Sun, Y.M. Song, et al., Topology synthesis of three-legged spherical parallel manipulators employing Lie group theory, Proceedings of the Institution of Mechanical Engineers, Part C: Journal of Mechanical Engineering Science 229 (10) (2015) 1873-1886.

[7] X.Y. He, Design and Kinematic Analysis of Single-Loop Multi-Mode Reconfigurable Mechanisms, Ph.D. Thesis, Heriot-Watt University, 2015.

[8] X.W. Kong, C.M. Gosselin, Type Synthesis of Parallel Mechanisms, Springer, Berlin, 2007.

[9] X.Y. He, X.W. Kong, D. Chablat, et al., Kinematic analysis of a single-loop reconfigurable 7R mechanism with multiple operation modes, Robotica 32 (7) (2014) 1171-1188.

[10] X.Y. He, X.W. Kong, G.B. Hao, et al., Design and analysis of a new 7R single-loop mechanism with 4R, 6R and 7R operation modes, Advances in Reconfigurable Mechanisms and Robots II, Mechanisms and Machine Science, Springer, Cham, 2016, pp. 27-37.

[11] C.C. Lee, J.M. Hervé, Generators of the product of two Schoenflies motion groups, European Journal of Mechanics-A/Solids 29 (1) (2010) 97-108.

[12] Q.C. Li, J.M. Hervé, Parallel mechanisms with bifurcation of Schoenflies motion, IEEE Transactions on Robotics 25 (1) (2009) 158-164.

[13] Q.C. Li, Z. Huang, J.M. Hervé, Type synthesis of 3R2T 5-DOF parallel mechanisms using the Lie group of displacements, IEEE Transactions on Robotics and Automation 20 (2) (2004) 173-180.

[14] C.C. Lee, J.M. Hervé, Translational parallel manipulators with doubly planar limbs, Mechanism and Machine Theory 41 (4) (2006) 433-455.

[15] C.C. Lee, J.M. Hervé, Isoconstrained parallel generators of Schoenflies motion, ASME Journal of Mechanisms and Robotics 3 (2) (2011) 021006-1-021006-10.

[16] X.W. Kong, C.M. Gosselin, Type synthesis of 3-DOF translational parallel manipulators based on screw theory, ASME Journal of Mechanical Design 126 (1) (2004) 83-92.

[17] X.W. Kong, C.M. Gosselin, Type synthesis of 3T1R 4-DOF parallel manipulators based on screw theory, IEEE Transactions on Robotics and Automation 20 (2) (2004) 181-190.

[18] S.F. Yang, T. Sun, T. Huang, et al., A finite screw approach to type synthesis of three-DOF translational parallel mechanisms, Mechanism and Machine Theory 104 (2016) 405-419.

[19] S.F. Yang, T. Sun, T. Huang, Type synthesis of parallel mechanisms having 3T1R motion with variable rotational axis, Mechanism and Machine Theory 109 (2017) 220-230.

[20] Z.M. Bi, Y. Jin, Kinematic modeling of Exechon parallel kinematic machine, Robotics and Computer-Integrated Manufacturing 27 (1) (2011) 186-193.

[21] T. Sun, S.F. Yang, T. Huang, et al., A way of relating instantaneous and finite screws based on the screw triangle product, Mechanism and Machine Theory 108 (2017) 75-82.

[22] J.S. Dai, Geometrical Foundations and Screw Algebra for Mechanisms and Robotics, Higher Education Press, Beijing, 2014. ISBN: 9787040334838 (translated from J.S. Dai, Screw Algebra and Kinematic Approaches for Mechanisms and Robotics, Springer, London, 2019.)

[23] J.S. Dai, Euler–Rodrigues formula variations, quaternion conjugation and intrinsic connections, Mechanism and Machine Theory 92 (2015) 144-152.

[24] J.S. Dai, Finite displacement screw operators with embedded Chasles' motion, ASME Journal of Mechanisms and Robotics 4 (4) (2012) 041002-1-041002-9.

[25] J.S. Dai, An historical review of the theoretical development of rigid body displacements from Rodrigues parameters to the finite twist, Mechanism and Machine Theory 41 (1) (2006) 41-52.

[26] J.S. Dai, N. Holland, D.R. Kerr, Finite twist mapping and its application to planar serial manipulators with revolute joints, Proceedings of the Institution of Mechanical Engineers, Part C: Journal of Mechanical Engineering Science 209 (4) (1995) 263-271.

[27] T. Sun, X.M. Huo, Type synthesis of 1T2R parallel mechanisms with parasitic motions, Mechanism and Machine Theory 128 (2018) 412-428.

[28] Y.M. Song, H. Gao, T. Sun, et al., Kinematic analysis and optimal design of a novel 1T3R parallel manipulator with an articulated travelling plate, Robotics and Computer-Integrated Manufacturing 30 (5) (2014) 508-516.

[29] Y.M Song, B.B. Lian, T. Sun, et al., A novel five-degree-of-freedom parallel manipulator and its kinematic optimization, ASME

Journal of Mechanisms and Robotics 6 (4) (2014), 041008-1-041008-9.
[30] T. Sun, Y.M. Song, Y.G. Li, et al., Workspace decomposition based dimensional synthesis of a novel hybrid reconfigurable robot, ASME Journal of Mechanisms and Robotics, 2 (3) (2010) 031009-1-031009-8.
[31] Y.M. Li, Q.S. Xu, Kinematic analysis of a 3-PRS parallel manipulator, Robotics and Computer-Integrated Manufacturing 23 (4) (2007) 395-408.
[32] Y.M. Li, Q.S. Xu, Design and development of a medical parallel robot for cardiopulmonary resuscitation, IEEE/ASME Transactions on Mechatronics 12 (3) (2007) 265-273.
[33] T. Sun, B.B. Lian, Y.M. Song, et al., Elastodynamic optimization of a 5-DoF parallel kinematic machine considering parameter uncertainty, IEEE/ASME Transactions on Mechatronics 24 (1) (2019) 315-325.
[34] Y.M. Li, Q.S. Xu, Dynamic modeling and robust control of a 3-PRC translational parallel kinematic machine, Robotics and Computer-Integrated Manufacturing 25 (3) (2009) 630-640.
[35] Y.M. Li, Y.G. Liu, X.P. Liu, et al., Parameter identification and vibration control in modular manipulators, IEEE/ASME Transactions on Mechatronics 9 (4) (2004) 700-705.
[36] T. Sun, Y.P. Zhai, Y.M. Song, et al., Kinematic calibration of a 3-DoF rotational parallel manipulator using laser tracker, Robotics and Computer-Integrated Manufacturing 41 (2016) 78-91.
[37] B.B. Lian, T. Sun, Y.M. Song, Parameter sensitivity analysis of a 5-DoF parallel manipulator, Robotics and Computer-Integrated Manufacturing 46 (2017) 1-14.
[38] T. Sun, B.B. Lian, Stiffness and mass optimization of parallel kinematic machine, Mechanism and Machine Theory 120 (2018) 73-88.
[39] T. Sun, H. Wu, B.B. Lian, et al., Stiffness modeling, analysis and evaluation of a 5 degree of freedom hybrid manipulator for friction stir welding, Proceedings of the Institution of Mechanical Engineers, Part C: Journal of Mechanical Engineering Science 231 (23) (2017) 4441-4456.
[40] T. Sun, B.B. Lian, Y.M. Song, Stiffness analysis of a 2-DoF over-constrained RPM with an articulated traveling platform, Mechanism and Machine Theory 96 (2016) 165-178.
[41] B.B. Lian, T. Sun, Y.M. Song, et al., Stiffness analysis and experiment of a novel 5-DoF parallel kinematic machine considering gravitational effects, International Journal of Machine Tools and Manufacture 95 (2015) 82-96.
[42] T. Sun, D. Liang, Y.M. Song, Singular-perturbation-based nonlinear hybrid control of redundant parallel robot, IEEE Transactions on Industrial Electronics 65 (4) (2018) 3326-3336.
[43] D. Liang, Y.M. Song, T. Sun, et al., Rigid-flexible coupling dynamic modeling and investigation of a redundantly actuated parallel manipulator with multiple actuation modes, Journal of Sound and Vibration 403 (2017) 129-151.
[44] D. Liang, Y.M. Song, T. Sun, et al., Optimum design of a novel redundantly actuated parallel manipulator with multiple actuation modes for high kinematic and dynamic performance, Nonlinear Dynamics 83 (2016) 631-658.
[45] J.S. Dai, Z. Huang, H. Lipkin, Mobility of overconstrained parallel mechanisms, ASME Journal of Mechanical Design 128 (1) (2004) 220-229.
[46] J.S. Dai, J.R. Jones, Mobility in metamorphic mechanisms of foldable/erectable kinds, ASME Journal of Mechanical Design 121 (3) (1999) 375-382.
[47] J.S. Dai, J.R. Jones, Null–space construction using cofactors from a screw–algebra context, Proceedings of the Royal Society A-Mathematical, Physical and Engineering Sciences 458 (2024) (2002) 1845-1866.
[48] J.S. Dai, J.R. Jones, Interrelationship between screw systems and corresponding reciprocal systems and applications, Mechanism and Machine Theory 36 (5) (2001) 633-651.
[49] J.S. Dai, J.R. Jones, Mobility in metamorphic mechanisms of foldable/erectable kinds, ASME Journal of Mechanical Design 121 (3) (1999) 375-382.